Experimental Studies on a Four-Way Microwave Power Combining System Based on Hybrid Injection-Locked 20-kW S-Band Magnetrons

Zhenlong Liu, Xiaojie Chen, Menglin Yang, Pengde Wu, Kama Huang, and Changjun Liu, *Senior Member, IEEE*

***Abstract*— A microwave power combining system based on four 20-kW hybrid injection-locked magnetrons in the S-band was proposed and presented. A high-power-capacity power combiner was designed, and the behaviors of the hybrid injection-locking magnetrons were qualitatively explained. An excellent output amplitude stability of 0.01 dB (peak-to-peak), a phase stability of ±0.9° (peak-to-peak), and a spur suppression ratio of −65.0 dBc at 500 kHz were achieved when the injection ratio was 0.07. The proposed four-way 20-kW magnetron coherent power combining system exhibits a total output power of over 60.6 kW and a combining efficiency of 91.5%. Simultaneously, neither real-time automatic phase tuning processes nor high-isolation circulators are required in the system. The results show that a high-efficiency magnetron power combining system has the potential to be applied as a cost-effective high-power microwave source for industrial applications. To the best of the authors' knowledge, a microwave power combining system featuring four 20-kW S-band continuous wave magnetrons has been successfully testified for the first time. The power output of over 60.0 kW and combining efficiency of 91.5% set a new performance record for S-band magnetron power combining systems and represent the best phase noise performance reported for any injection-locked magnetron with an output power of over 15 kW.**

***Index Terms*— Injection-locking, magnetron, microwave power combining, phase.**

I. Introduction

HIGH-POWER microwaves have aroused tremendous interest in several industries (particularly in the field of chemical synthesis) [1], due to their fast reaction rate [2], high processing efficiency [3], and energy conservation properties [4]. However, the performance of high-power continuous-wave (CW) microwave generators or systems have not lived up to industrial expectations [5], although the high average power source could potentially be implemented by advanced techniques. For example, Kobayashi *et al.* [6] proposed an S-band 1-kW-class solid-state power amplifier for wireless space applications with a drain efficiency of 57% and a power combining efficiency of 87%. The Communications & Power Industries Company achieved a CW klystron with an output power of 500 kW at a single frequency of 2.114 GHz and a direct-current to microwave conversion efficiency of nearly 48% in the S-band [7]. Although these high-power CW sources are excellent in a variety of military applications, they are expensive, have low efficiency, and thus are not ideal candidates for industrial heating applications. On the other hand, the power capacity of a single-microwave source is ultimately limited by the restrictions of its cavity size, which is limited by the operational microwave frequency, e.g., the power capacity of a single-CW magnetron may reach 100 kW at 915 MHz and drop to 30 kW at 2.45 GHz [8]. To effectively solve the aforementioned problem, power combining of multiple oscillators is actively being pursued, particularly when the components of each oscillator are robust, low-cost, and highly efficient. One recommended oscillator for power combining in industry is the magnetron, which has low manufacturing costs and an efficiency exceeding 80%.

Magnetrons, although widely employed in industrial reactor systems, are regarded as noisy oscillators whose amplitude and phase randomly fluctuate. A fascinating proposal for solving the poor noise performance problem of magnetrons and combining multiple magnetrons under phase control is injection-locking technology. This solution is especially interesting for industrial processing, where amplitude and phase should be stabilized in an economical fashion. Shinohara *et al.* [9] discussed multiple magnetron power combining systems to achieve high-power outputs for a solar power station/satellite. Liu *et al.* [10] achieved a successful microwave power combination of two magnetrons using injection locking to obtain an output power of 25 kW with a 96% combining efficiency. However, both groups emphasized that the injection power should be high enough to search the overlapping locking frequency for coherent power combining, and a real-time phase controlling process should be employed to keep the combining efficiency and output power high. In addition, a microwave power combining system in industry is expected to be simpler and stabilize the amplitude and phase of the microwave output for reproducibility.

In this paper, we proposed a novel four-way microwave power combining method based on hybrid injection-locked

Manuscript received April 24, 2018; revised July 17, 2018; accepted October 14, 2018. Date of publication November 15, 2018; date of current version January 8, 2019. This work was supported in part by the National Basic Research Program of China (973 Program) under Grant 2013CB328902 and in part by the National Natural Science Foundation of China under Grant 61271074. The review of this paper was arranged by Senior Editor D. A. Shiffler. *(Corresponding author: Changjun Liu.)*

The authors are with the School of Electronics and Information Engineering, Sichuan University, Chengdu 610064, China (e-mail: cjliu@ieee.org).

Color versions of one or more of the figures in this paper are available online at http://ieeexplore.ieee.org.

Digital Object Identifier 10.1109/TPS.2018.2876574

magnetrons, and an experimental four-way 20-kW S-band magnetron power combining system was designed, built, and measured for the first time. The behaviors of the hybrid injection-locking magnetrons were qualitatively explained based on Adler's condition. A low-loss combiner was designed, and its phase relationship together with the resultant power combining efficiency of four magnetrons was analyzed. An investigation of the phase, amplitude stability, and spectral purity of the microwave power system output was also performed. To the best of the authors' knowledge, a successful microwave power combining system composed of four 20-kW S-band CW magnetrons was established for the first time. This exhibits some of the highest CW power outputs, combining efficiencies and phase noise performances ever reported for an S-band magnetron power combining system.

II. Theory and Analysis

A. Lossless Power Combiner

To achieve four-way microwave power combining, a 3-dB E-plane T-junction (E-T) was employed to unite two 3-dB H-plane T-junctions (H-T) as a five-port combiner, and both E-plane and H-plane T-junctions were designed with output impedance matching. The scattering matrix of a lossless 3-dB E-T and H-T power combiner with perfect impedance matching at the output port could be the form of (1) [11]. Ports 1 and 2 are the two input ports of the T-junction combiner, and port 3 is the output port

$$[S]_{H-\mathrm{T}} = \begin{bmatrix} \frac{1}{2} & -\frac{1}{2} & -\frac{j}{\sqrt{2}} \\ -\frac{1}{2} & \frac{1}{2} & -\frac{j}{\sqrt{2}} \\ -\frac{j}{\sqrt{2}} & -\frac{j}{\sqrt{2}} & 0 \end{bmatrix}$$
$$[S]_{E-\mathrm{T}} = \begin{bmatrix} \frac{1}{2} & \frac{1}{2} & -\frac{j}{\sqrt{2}} \\ \frac{1}{2} & \frac{1}{2} & \frac{j}{\sqrt{2}} \\ -\frac{j}{\sqrt{2}} & \frac{j}{\sqrt{2}} & 0 \end{bmatrix}. \tag{1}$$

The five-port combiner can be represented by a 5×5 scattering matrix, as shown in (2). According to the above E-T/H-T scattering matrices [12], it is easy to conclude that the five-port matrix should be reciprocal, symmetric, and lossless. The resulting five-port combiner scattering parameter will satisfy the requirements in (2) [13]. Ports 1 and 2 are input ports of one H-T combiner, ports 3 and 4 are inputs ports of the other H-T combiner, and port 5 is the output port

$$\begin{aligned} [S] &= \begin{bmatrix} S_{11} & S_{12} & S_{13} & S_{14} & S_{15} \\ S_{21} & S_{22} & S_{23} & S_{24} & S_{25} \\ S_{31} & S_{32} & S_{33} & S_{34} & S_{35} \\ S_{41} & S_{42} & S_{43} & S_{44} & S_{45} \\ S_{51} & S_{52} & S_{53} & S_{54} & S_{55} \end{bmatrix} \\ S_{55} &= 0 \\ S_{15} &= S_{51} = S_{25} = S_{52} = -1/2 \\ S_{35} &= S_{53} = S_{45} = S_{54} = 1/2 \\ S_{13} &= S_{31} = S_{14} = S_{41} = S_{23} \\ &= S_{32} = S_{24} = S_{42} = 1/4 \\ |S_{11}|^2 + |S_{12}|^2 &= |S_{22}|^2 + |S_{21}|^2 = 3/8 \\ |S_{33}|^2 + |S_{34}|^2 &= |S_{44}|^2 + |S_{43}|^2 = 3/8. \end{aligned} \tag{2}$$

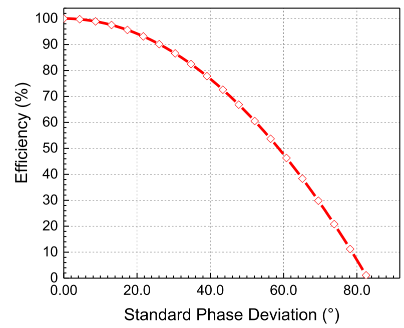

Fig. 1. Power combining efficiency with different standard phase deviations.

Assuming the input signals are $(P_i)^{1/2} \cdot e^{j\varphi_i} (i = 1, 2, 3, 4)$, and P_i and φ_i are the input power and phase of the combiner, respectively, the total power out P_t and the combining efficiency η are

$$\begin{aligned} P_\mathrm{t} &= \left| \sum_{i=1}^{4} S_{5i} \cdot \sqrt{P_i} e^{j\varphi_i} \right|^2 \\ \eta &= \frac{P_\mathrm{t}}{\sum_{i=1}^{4} P_i} \times 100\%. \end{aligned} \tag{3}$$

Thus, we can obtain the exact combining output power and efficiency from (3). The results illustrate that efficient power combining requires good matching of the input amplitude and phase characteristics, and the highest efficiency can be attained when the input amplitudes are equal and the phases satisfy $\varphi_1 = \varphi_2 = (\varphi_3 - \pi) = (\varphi_4 - \pi)$.

Liu *et al.* [10] show that the power combining efficiency is greater than 95%, even if the input power unbalance reaches 3 dB, and that an average output power of the high-power magnetron could be controlled by adjusting the anode current in the magnetron system [14]. Therefore, the phase balance should play a chief role in impairing power combining efficiency. To obtain a quick estimate of the relation between the power combining efficiency and phase difference, we assume that the magnetrons have an average output P and a Gaussian distribution in a total phase jitter (φ_1, φ_2, $\varphi_3 - \pi$, and $\varphi_4 - \pi$) with a standard phase deviation of Φ. Thus, the combined power and efficiency should be simplified as [15]

$$\begin{aligned} P_\mathrm{t} &= 4P \left(1 - \frac{3}{2} \cdot \frac{\Phi^2}{\pi} \right) \\ \eta &= 1 - \frac{3}{2} \cdot \frac{\Phi^2}{\pi}. \end{aligned} \tag{4}$$

The power combining efficiency with respect to a different standard phase deviation, as calculated from (4), is shown in Fig. 1. Clearly, the larger the standard phase deviation is, the lower the power combining efficiency should become. It can be quickly deduced that when $\Phi \leq 26°$, the power combining efficiency is greater than 90%, and no combining effect can occur when $\Phi = 71.8°$. However, the phase of a free-running magnetron varies dramatically between $-180°$ and $180°$ [10]; thus, the hybrid injection-locked magnetron is introduced for phase control to obtain a high-power combining efficiency.

B. Hybrid Injection-Locked Magnetron

The matrix in (2) illustrates that the input ports of the five-port power combiner lack isolations [13], and the circulators have deteriorated and cannot isolate such couplings effectively when the magnetron output power is sufficiently high. As a result, mutual couplings exist to affect the magnetron output frequency and phase. The instantaneous output frequency and phase of four-way mutual coupling magnetrons are represented by the following equations [16], [17]:

$$\omega_{\text{out}} = \omega_i + \frac{d\varphi_i}{dt} \tag{5}$$

$$\frac{d\varphi_i}{dt} = (\omega_i - \omega_{\text{out}}) + \sum_{j=1, j\neq i}^{4} \frac{\xi_{i,j}\omega_i}{2Q_i}\sin(\varphi_j - \varphi_i) \quad (i = 1, 2, 3, 4) \tag{6}$$

where ω_i and ω_{out} are the frequency of the ith free-running magnetron output and the mutual coupling output, respectively; $\xi_{i,j} = (P_{i,j}/P_i)^{1/2}$ is the coupling strength; $P_{i,j}$ is the power of the ith magnetron coupling from jth magnetron; P_i is the ith magnetron output power; φ_i, and φ_j are the self-excitation phases of the respective magnetron; and Q_i is the external Q of the magnetron.

The high-efficiency power combining requires a constant phase between any two magnetron outputs, such that $\varphi_i - \varphi_j = \Delta\varphi$ for $i \neq j$. The mutual couplings are reciprocal and symmetric ($\xi_{1,3} = \xi_{2,4} = \xi_{3,1} = \xi_{4,2} = \xi$; $\xi_{1,2} = \xi_{3,4} = \xi_{2,1} = \xi_{4,3} = \xi'$), and the phase shift $\Delta\varphi$ between the actual mutual locked magnetrons is restricted to the range of $-\pi/2 < \Delta\varphi < \pi/2$ [14]. Similar to [18], it is assumed that the external Q factors of the magnetrons are equal, a constant phase progression $\varphi_1 = \varphi_2 = (\varphi_3 - \pi/2) = (\varphi_4 - \pi/2)$ can be synthesized at a frequency ω_{out} by the following free-running frequencies distribution:

$$\begin{aligned} \omega_1 &= \omega_2 \approx \omega_3 + 2\Delta\omega \approx \omega_4 + 2\Delta\omega \\ \omega_{\text{out}} &= \omega_1 - \Delta\omega \\ \Delta\omega &= \xi\omega_1/Q. \end{aligned} \tag{7}$$

According to Slater [19], the frequency of a free running magnetron in this instance is given by

$$\omega_i = \omega_0 - \frac{B}{2Q}\omega_0 + \frac{b}{2C}. \tag{8}$$

Here, the magnetron resonance cavity is equivalent to the lumped *RLC* circuit; the characteristics of the electronic discharge and electronic interactions are represented by the conductance g and susceptance b; the external load is described by the load conductance G and conductance B; Q is the external loaded quality factor of the magnetron; $\omega_0 = (LC)^{1/2}$ is the resonance frequency; and ω_i is the instantaneous angular frequency of the magnetron.

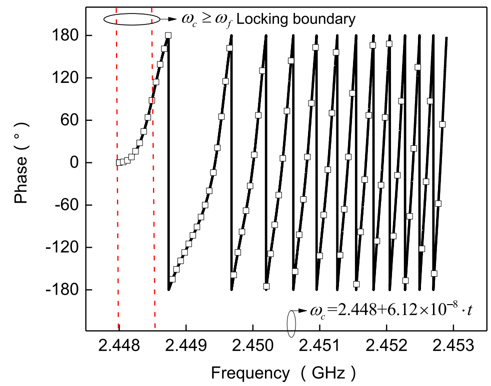

Fig. 2. Output phases in comparison to the coupling frequencies.

As indicated from (8), the free-running frequency control can be easily acquired by changing the reactance of the load into that in which the magnetron operates. Therefore, three 3-stub tuners were used to tune the required free-running frequencies distribution of magnetrons, as shown in Fig. 3.

To clearly illustrate the phase behaviors with a frequency difference, we draw the line charts by solving (6), as shown in Fig. 2, with some assumed parameters. Specifically, $\varphi_1 = \varphi_2$, $\varphi_3 = \varphi_4$, ξ/Q is 0.000243, the free-running magnetron's frequency ($\omega_3 = \omega_4 = \omega_{\text{f}}$) is 2.448 GHz, and the coupling frequency ($\omega_1 = \omega_2 = \omega_{\text{c}}$) is 2.448 GHz and then assumed to increase linearly over time, as shown in Fig. 2. Fig. 2 illustrates that if the mutual coupling frequency differences are neglected, the magnetron output phase is 0, and if the coupling frequency increases with the locking range, the output phase increases as well, and vice versa. Once the coupling frequency is out of the locking range, the magnetron output phase uniformly distributes between $\pm\pi$.

Thus, we can conclude that the input phase of the above-mentioned five-port power combiner satisfies $\varphi_1 = \varphi_2 = (\varphi_3 - \pi/2) = (\varphi_4 - \pi/2)$, and no combining effect occurs when mutual locking tunes to the mentioned frequencies in (7). Moreover, although Adler's condition is satisfied, the magnetron output phase is roughly a constant or still jittering because it is in the presence of fluctuations in the free-running magnetron frequency [20].

To overcome the drawbacks listed above, the external injection signals are directly injected to each magnetron, respectively, as shown in Fig. 3. Now, the magnetron is subjected to both external and mutual injections in the power combining system, which we now refer to as a hybrid injection magnetron. The criterion for hybrid injection locking is described following Adler's formula [21]:

$$\frac{\rho_i}{2Q} \geq \left|\frac{\omega_{\text{inj}} - \omega_{\text{out}}}{\omega_{\text{out}}}\right| \tag{9}$$

where $\rho = (P_{\text{inj}}/P_i)^{1/2}$ is the injection ratio, and ω_{inj} is the injected frequency.

Equation (9) shows the required power to lock a magnetron [22]. When Adler's condition is well satisfied, the magnetrons are completely locked at the external signal frequency, and we can compensate the output phase with an extra phase

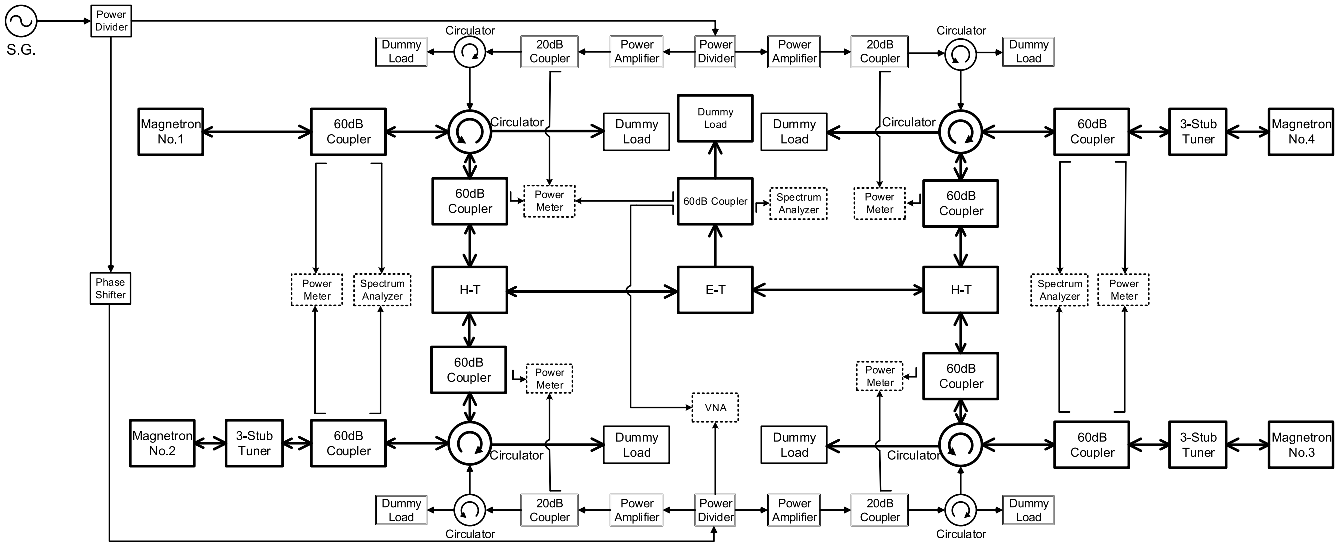

Fig. 3. Diagram of the 60-kW CW magnetron microwave power combining system. Dashed line framework part: measurement setup. Connected to signal generator (top and bottom) injection signal route. Highlighted middle part: high-power output route.

shifter. Consequently, the goal of the high-power combining efficiency can be successfully fulfilled through adjusting the compensate phase shifter to achieve the abovementioned phase condition of the five-port combiner ($\varphi_1 = \varphi_2 = \varphi_3 - \pi = \varphi_4 - \pi$).

Moreover, after the magnetron frequency is completely locked, the frequency can be controlled independently within the locking range.

III. Experimental System

The block diagram of a four-way 20-kW CW magnetron microwave power combining system based on WR430 waveguides is shown in Fig. 3. According to a schematic, we built the 60-kW CW magnetron microwave power combining system, the main hardware components of which are shown in Fig. 4. The cooling treatment system for water circulation is connected to magnetrons, circulators, and water-cooled dummy load, with the cooling tower not shown in Fig. 4.

The industrial magnetrons used for the power combining experiments were water-cooled CW CK-2091 magnetrons, which were manufactured by Nanjing Sanle Electronic Information Industry Group Co., Ltd., Nanjing, China. The magnetic field intensity of the magnetron was 1250 Gs, which was supplied by an extra electromagnet with an operating dc current of 3.2 A. The power supply of the magnetron was a dc switching power supply that maintained a voltage ripple of less than 1.5%. The preheating filament current required by the magnetron is 47.0 A. Once the output power of free-running magnetrons reached 15.0 kW, the cathode current was decreased to approximately 25.0 A to reduce the frequency modulation noise, which stabilized the oscillation to yield a narrowband spectrum [16]. In addition, the center frequency of the free-running magnetron was controlled by tuning the magnetron reflection coefficient with the help of a three-stub tuner (HD-22WST3, HD Microwave Co., Xi'an, China).

Fig. 4. Hardware setup for the 60-kW CW magnetron microwave power combining system. (1) Magnetron, electromagnet, and external excitation cavity. (2) 12-kV high-voltage power supply. (3) Filament power supply. (4) Three-stub tuner. (5) 60-dB coupler. (6) 30-kW four-port circulator. (7) 30-kW water-cooled dummy load. (8) H-T combiner. (9) E-T combiner. (10) 80-kW water-cooled dummy load. (11) 20-dB coupler. (12) Coaxial-to-waveguide adapter. (13) 5-kW three-port circulator. (14) 5-kW water-cooled dummy load. (15) 200-W power amplifier. (16) Power meter. (17) Signal analyzer. (18) Vector network analyzer. (19) Signal generator. (20) Phase shifter controlled computer. (21) Cooling treatment system for water circulation. (22) Monitoring industrial personal computer.

A signal generator (E8267C, Agilent) was split into two equiphase equiamplitude parts, and one of the split signal's phases was controlled by a digital USB phase shifter (TEP4000-5, Telemakus), which had a phase-adjusting range of 400° (typical) with a 0.25° resolution. Then, two equiamplitude signals divided into four parts were amplified with a 40-dB power amplifier (YYPA4D, Sanle Microwave Co., Nanjing) to provide the injection signals. The circulators (26WHPDPSC30KW, HD Microwave Co.) with the dummy loads (KT-22WWL30kW, KT Microwave Co., Nanjing) transmitted the injected signal to the magnetron and acted as isolators to protect both the magnetron and the amplifier. We designed two H-T's with a metal rod in the middle as the required dual magnetrons power combiner, and an E-T with a chamfer in the middle as the final total output power combiner. The total combining output microwave power was mainly absorbed by water-cooled dummy loads (Vacuum Electronics Research Institute, Beijing, China).

Nine 60-dB directional couplers (KT-22WDC60N60KW, KT Microwave Co.) were employed to sample the high-power microwave signals for the power measurements (power meter, AV2433, the 41st Institute of CETC), the spectrum and phase noise measurements (signal analyzer, FSV40, Rohde & Schwarz), as well as for the amplitude and phase measurements (vector network analyzer, E8362B, Agilent). Four 20-dB directional couplers (SLDC-20-7F-NF, Rosenberger Co., Fridolfing, Germany) were employed to sample the injection microwave signals for the power measurements.

IV. Results and Discussion

For a waveguide T-junction, the discontinuities of the waveguide (a metal rod or chamfer), which excite the higher order mode, have strong effects on insertion loss in a power combining network. To decrease the higher order mode effect and achieve the expected results, commercial 3-D electromagnetic simulation software based on a finite-difference time-domain method was employed for optimization. Since the power divider is reciprocal and symmetric, only the S-parameters of port 1 and S_{55} are presented.

The optimum simulated and experimental S parameters of the five-port power combiner are depicted in Fig. 5(a); the output port 5 of the power combiner was well matched because both the simulated and experimental return losses ($|S_{55}|$) were better than 20.0 dB. The transmission coefficient ($|S_{51}|$) was approximately -6.0 dB, and the insertion loss was less than 0.2 dB. The coupling between two different H-T input ports ($|S_{13}|$) was also approximately -12.0 dB. The reflection of the input port 1 ($|S_{11}|$) varied from -2.2 to -9.9 dB with increasing frequency, and the coupling between the same H-T input ports ($|S_{12}|$) changed in the opposite trend simultaneously. The simulated and experimental results of the five-port power combiner correspond to the theoretical values of (2).

Considering the hybrid injections, the combiner input phases satisfied the relations ($\varphi_1 = \varphi_2 = 0$ and $\varphi_3 = \varphi_4 = 165°$). The designed combiner was excited by four input signals, whose amplitudes were 20 kW, and the phase relations were $\varphi_1 = \varphi_2 = 0$ and $\varphi_3 = \varphi_4 = 165°$ simultaneously. The simulated S-parameter is shown in Fig. 5(b). The transmission coefficient ($|S_{51}|$) is the same as the S-parameter previously listed. All return losses ($|S_{11}|$ and $|S_{55}|$) were better than 16.0 dB, along with the isolation ($|S_{12}|$), which was better than 16.0 dB, and the isolation ($|S_{13}|$) was nearly the same as the abovementioned measured S-parameters. That is, the reflections of input ports mostly canceled out if the input signals satisfied the abovementioned assumption, and the remaining coupling parts, through the low-isolated circulators, acted as the mutual injection signals.

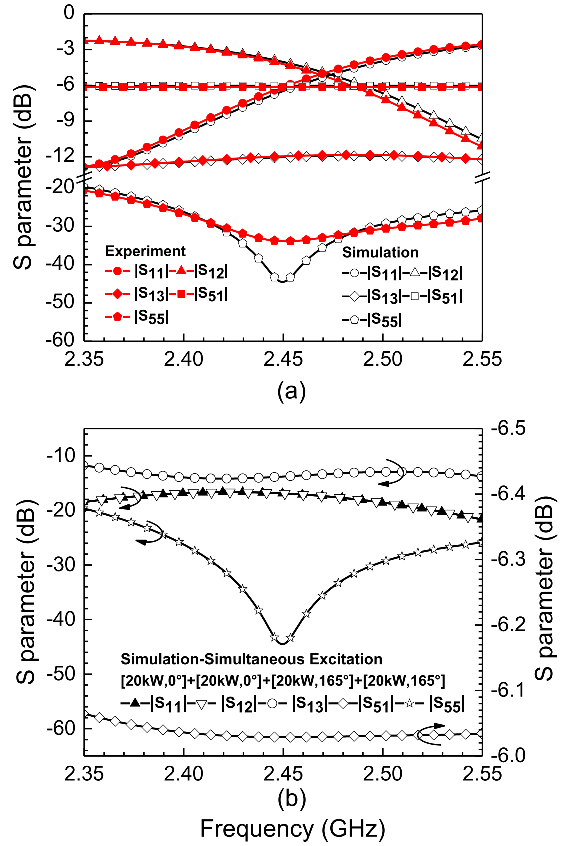

Fig. 5. (a) Simulated and experimental S-parameter of the five-port power combiner. (b) Simulated S-parameter of the desired input amplitudes and phases.

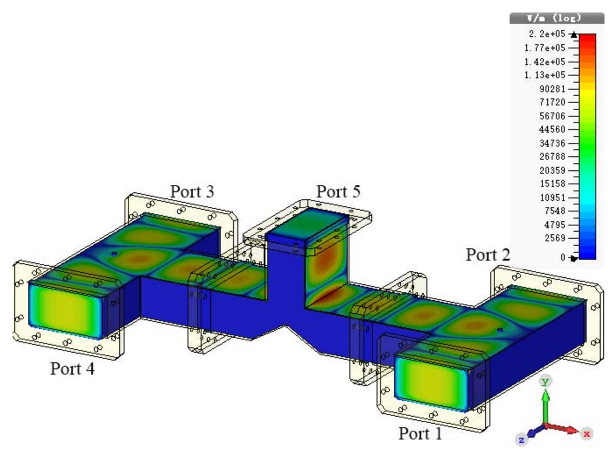

Fig. 6. E-field distribution for the four-way power combining with an incident power of 80 kW.

The electric field distributions with a total incident power of 80 kW and the above phase relations are shown in Fig. 6. The electric field distribution was symmetrical, and the output electric field intensity was twice as high as the input signal. The maximum surface electric field appeared at the output E-T branch and was approximately 220.0 kV/m, which was much lower than the breakdown threshold of 30 kV/cm for CW operation [23]. Thus, the five-port power combiner can be directly used for a power combining system, and the

TABLE I
EXPERIMENTAL RESULTS OF POWER COMBINING

Frequency (GHz)	Magnetron Output Power (kW)				Five-port Combiner Input Power (kW)				Total Output Power (kW)	Combining Efficiency	DC to Microwave Efficiency
2.4479	19.9	16.8	19.3	16.7	18.1	15.3	17.6	15.2	60.6	91.5%	61.3% (1)
2.4476	19.9	16.8	19.3	16.7	18.1	15.3	17.6	15.2	60.9	93.1%	62.3% (1)
2.4470	19.9	16.8	19.3	16.7	18.1	15.3	17.6	15.2	61.6	93.1%	62.3% (1)
2.4460	12.7	14.4	13.1	13.0	11.6	12.6	12.1	11.9	45.1	93.5%	58.2% (2)

(1) When the microwave output power is greater than 60 kW, the DC power levels of the four magnetrons are 26.58 kW, 22.68 kW, 27.00 kW, and 22.59 kW.
(2) When the microwave output power is greater 40 kW, the DC power levels of the four magnetrons are 18.14 kW, 19.90 kW, 19.40 kW, and 19.97 kW.

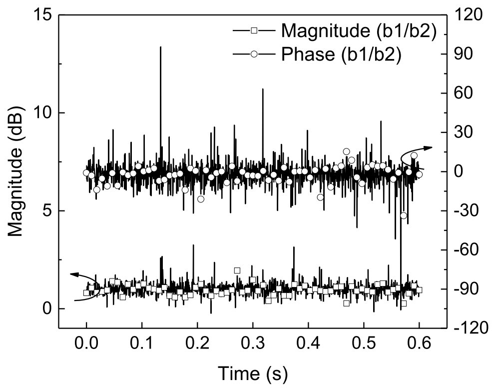

Fig. 7. Amplitude and phase difference of magnetron No. 1 and No. 2 with the above frequency distribution.

calculated highest resultant power combining efficiency was higher than 95.0%, which corresponds to the values estimated using (4).

The initial output behaviors of four magnetrons were measured separately. The initial self-oscillation frequency of the four magnetrons oscillated at 2.44865 (anode voltage of −12.60 kV and anode current of 2.11 A), 2.44967 (anode voltage of −12.60 kV and anode current of 1.80 A), 2.4470 (anode voltage of −11.59 kV and anode current of 2.33 A), and 2.44542 GHz (anode voltage of −11.89 kV and anode current of 1.90 A), and the corresponding average powers of the four magnetrons' output were 19.91, 16.83, 19.36, and 16.72 kW, respectively.

The free-running frequency of magnetron No. 1 was set as the reference frequency (ω_0) because there was no three-stub tuner in series with the magnetron, as shown in Fig. 3. Based on the analysis of the hybrid injection-locked magnetron, the center frequency of the free-running magnetron should satisfy a frequency distribution of $\omega_1 = \omega_2 = \omega_0$ and $\omega_3 = \omega_4 = \omega_0 - 2\Delta\omega$. Magnetron No. 3 or No. 4 received the coupling power from magnetron No. 1, which was 26.4 W. For $Q \approx 115$, $\Delta\omega$, which was estimated by (7), was approximately equal to 0.75 MHz. With careful tuning of the three-stub tuners, the required reflection coefficient of the magnetron was obtained, and the self-oscillation frequency of the four magnetrons oscillated at 2.44865, 2.44870, 2.44723, and 2.44710 GHz, respectively.

When all four magnetrons operated in the power combining system, the frequency was synthesized at 2.4481 GHz, which was close to the value predicted via (7). A vector network analyzer was used to monitor the amplitude and phase difference between magnetrons No. 1 and No. 2 at the synthesized frequency. Fig. 7 shows the measured amplitude and phase shift for approximately 600 ms. Unlike a free-running magnetron whose amplitude fluctuates violently, the above peak-to-peak amplitude was less than ± 1.5 dB; the center of the phase difference was 0°, and the peak-to-peak phase shift of the magnetron output was reduced from $\pm 180°$ (free-running mode) peak-to-peak to $\pm 120°$ (mutual injection mode) peak–to-peak. The phase and amplitude jitter were mainly caused by the weak couplings and frequency chirps of the free-running operation. Other magnetrons depicted the same behavior, but the center of the phase difference between magnetron No. 1 or No. 2 and No. 3 or No. 4 was less than 90°, as the isolations of the combiner were deteriorated by unsatisfied phase conditions. Such behaviors are consistent with the previous analysis, but the total output was only 18.9 kW, and no combining effect occurred. The external injection should be employed to compensate phases.

The decreased amplitude and phase jitters of the magnetron in the current system are no doubt likely to reduce the external injection power and increase stability [20]. Considering the long-time stability and output locking bandwidth, the injection power was determined to be 100 W, whereas the injection ratio was 0.07, much lower than that reported in [10]. Thus, all the magnetrons were injected, and an extra phase shifter was employed to compensate for the phase difference. The microwave power combining achieved the highest output power and a high efficiency when the phase compensation was completed.

Table I shows the experimental results of the microwave power combining based on four hybrid injection-locked 20-kW CW magnetrons. The insertion loss of the circulators should be taken into consideration in Table I as well. The output power and efficiency exceed 60.6 kW and 91.5%, respectively. The efficiency of power combining, which is lower than the simulation value, is mainly caused by the insertion loss of the combiner and reflections of the water cooled dummy load. It is noted that such reflections are reinjected to magnetrons to enhance this optimum state. The total dc to microwave efficiency reaches up to 61.3%. Under the same conditions, the microwave output power decreased as the anode current of the magnetron decreased, but the power combining efficiency was still 93.5%; the total dc to microwave efficiency

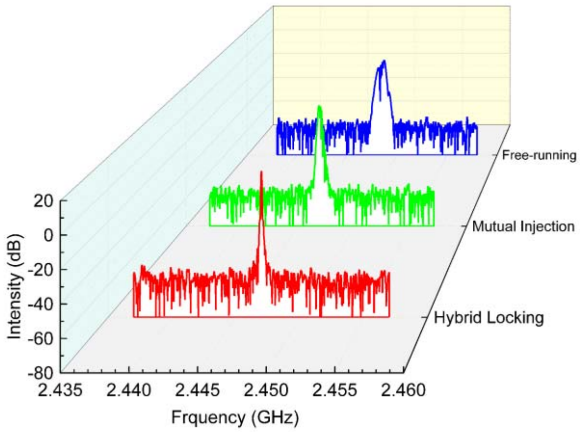

Fig. 8. Spectra of the magnetron's output in different states (RBW of 50 kHz and VBW of 50 kHz).

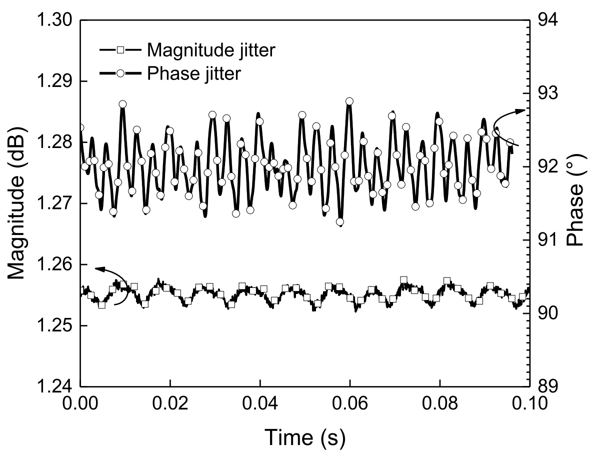

Fig. 9. Relative amplitude and phase jitters of the total output.

decreased to 58.2%, which was caused by the decrease in the dc-microwave conversion efficiencies of the magnetrons.

Fig. 8 shows the spectrum of the magnetron's output characteristics at different states. Fig. 8 shows that random frequency fluctuations are visible in the characteristics during the free-running operation and that the spectrum of the free-running magnetron may shift with respect to time. The mutual injection magnetron showed no frequency variation, a relatively sharp frequency spectrum and a distinct frequency chirp on the right side of its spectrum, which was caused by weak couplings and jitters of the self-excitation frequency. When hybrid locking was achieved, all microphonic signals and frequency chirps disappeared, and the frequency spectrum was sharper than that in the abovementioned states. Furthermore, all background noise was lower than −53.0-and −50.0-dB oscillation spectrum width was calculated to illustrate spectrum improvement. The spectrum widths were 2.500, 1.250, and 0.625 MHz from the free-running operation to the hybrid locking state, respectively; the final output spur suppression improved visibly, and the spur suppression ratio was measured to be −65.0 dBc at 500 kHz. Both the spectrum widths and the spur suppression ratio show significant improvements compared with the values reported in [10], [24], and [25].

The amplitude and phase jitters between the total combining output and reference signal source output were measured by a vector network analyzer, as shown in Fig. 3. Fig. 9 shows the measured relative amplitude and phase jitter of total output at approximately 100 ms. The peak-to-peak amplitude was nearly constant (less than 0.01-dB peak-to-peak), and the peak-to-peak phase shift of the output was reduced from ±120° (mutual injection) peak-to-peak to ±0.9° (hybrid injection-locking) peak–to-peak, which coincided well with the previous estimation. We also demonstrated that the amplitude and phase jitters in the current system could be attributed to fluctuations of the dc power supply because the period of the amplitude and phase jitters and the rectified mains ripple remained consistent [26].

V. Conclusion

A four-way 20-kW S-band magnetron power combining system without a real-time automatic phase tuning process and high-isolation circulators was proposed, built, and measured for the first time. A high-power-capacity combiner was designed, and the behaviors of the hybrid injection-locking magnetrons were qualitatively explained. An excellent output amplitude stability of 0.01 dB (peak-to-peak), a phase stability of ±0.9° (peak-to-peak), and a spur suppression ratio of −65.0 dBc at 500 kHz were achieved at an injection ratio of 0.07. The proposed four-way 20-kW magnetron coherent power combining system exhibited a total output power of over 60.6 kW and a combining efficiency of 91.5%. Moreover, few expensive components were employed in our microwave power system, such as an electrically controlled phase shifter. The experimental results show that a high-efficiency magnetron power combining system has the potential to be applied as a cost-effective, high-power microwave source for industrial applications. To the best of the authors' knowledge, a microwave power combining system composed of four 20-kW S-band CW magnetrons has been successfully demonstrated for the first time. This system produces some of the highest CW power outputs, combining efficiencies and phase noise performances ever reported for an S-band magnetron power combining system.

References

[1] C. Shibata, H. Tamai, T. Tanaka, and M. Wakamatsu, "High-power (500-kW) CW magnetron for microwave heating," *Elect. Eng. Jpn.*, vol. 111, no. 2, pp. 94–101, 1991.

[2] H. Shang, C. E. Snape, S. W. Kingman, and J. P. Robinson, "Treatment of oil-contaminated drill cuttings by microwave heating in a high-power single-mode cavity," *Ind. Eng. Chem. Res.*, vol. 44, no. 17, pp. 6837–6844, Jul. 2005.

[3] J. D. Moseley and C. O. Kappe, "Cheminform abstract: A critical assessment of the greenness and energy efficiency of microwave-assisted organic synthesis," *Green Chem.*, vol. 13, no. 4, pp. 794–806, 2011.

[4] S. L. Yao, E. Suzuki, N. Meng, and A. Nakayama, "A high-efficiency reactor for the pulsed plasma conversion of methane," *Plasma Chem. Plasma Process.*, vol. 22, no. 2, pp. 225–237, 2002.

[5] M. Vollmer, "Physics of the microwave oven," *Phys. Educ.*, vol. 39, no. 1, p. 74, 2004.

[6] Y. Kobayashi, S. Yoshida, Z.-I. Yamamoto, and S. Kawasaki, "S-band GaN on Si based 1kW-class SSPA system for space wireless applications," *IEICE Trans. Electron.*, vol. E96.C, no. 10, pp. 1245–1253, 2013.

[7] W. W. Shelton, "Development of high power microwave devices for use in bioeffects studies," Bioeng. Res. Centre, Georgia Inst. Technol., Atlanta, GA, USA, Tech. Rep. B-03-A13, 1990.

[8] S. K. Vyas, S. Maurya, and V. P. Singh, "Electromagnetic and particle-in-cell simulation studies of a high power strap and vane CW magnetron," *IEEE Trans. Plasma Sci.*, vol. 42, no. 10, pp. 3373–3379, Oct. 2014.

[9] N. Shinohara, H. Matsumoto, and K. Hashimoto, "Solar power station/satellite (SPS) with phase controlled magnetrons," *IEICE Trans. Electron.*, vol. E86-C, no. 8, pp. 1550–1555, 2003.

[10] C. Liu, H. Huang, Z. Liu, F. Huo, and K. Huang, "Experimental study on microwave power combining based on injection-locked 15-kWS-band continuous-wave magnetrons," *IEEE Trans. Plasma Sci.*, vol. 44, no. 8, pp. 1291–1297, Aug. 2016.

[11] J. Ruiz, P. Soto, V. E. Boria, and A. A. S. Bias, "Compensated double-ridge waveguide E-plane and H-plane T-junctions," in *Proc. 15th Medit. Microw. Symp. (MMS)*, Nov./Dec. 2015, pp. 1–4.

[12] D. M. Pozar, *Microwave Engineering*. Hoboken, NJ, USA: Wiley, 2009.

[13] O. R. Price and M. Leichter, "Scattering matrix for an N-Port power-divider junction," *IEEE Trans. Microw. Theory Techn.*, vol. MTT-8, no. 6, p. 669, Nov. 1960.

[14] N. Shinohara and H. Matsumoto, "Research on magnetron phased array with mutual injection locking for space solar power satellite/station," *Elect. Eng. Jpn.*, vol. 173, no. 2, pp. 21–32, Nov. 2010.

[15] S. E. Kubasek, D. M. Goebel, W. L. Menninger, and A. C. Schneider, "Power combining characteristics of backed-off traveling wave tubes for communications applications," *IEEE Trans. Electron Devices*, vol. 50, no. 6, pp. 1537–1542, Jun. 2003.

[16] F.-K. Wang *et al.*, "A novel vital-sign sensor based on a self-injection-locked oscillator," *IEEE Trans. Microw. Theory Techn.*, vol. 58, no. 12, pp. 4112–4120, Dec. 2010.

[17] R. A. York and T. Itoh, "Injection- and phase-locking techniques for beam control [antenna arrays]," *IEEE Trans. Microw. Theory Techn.*, vol. 46, no. 11, pp. 1920–1929, Nov. 1998.

[18] R. A. York and R. C. Compton, "Quasi-optical power combining using mutually synchronized oscillator arrays," *IEEE Trans. Microw. Theory Techn.*, vol. 39, no. 6, pp. 1000–1009, Jun. 1991.

[19] J. C. Slater, "The phasing of magnetrons," Res. Lab. Electron., MIT, Cambridge, MA, USA, Tech. Rep. 35, 1947.

[20] P. Pengvanich, Y. Y. Lau, J. W. Luginsland, R. M. Gilgenbach, E. Cruz, and E. Schamiloglu, "Effects of frequency chirp on magnetron injection locking," *Phys. Plasmas*, vol. 15, no. 7, p. 073110, Jul. 2008.

[21] R. Adler, "A study of locking phenomena in oscillators," *Proc. IEEE*, vol. 61, no. 10, pp. 1380–1385, Oct. 1973.

[22] P. Pengvanich *et al.*, "Modeling and experimental studies of magnetron injection locking," *J. Appl. Phys.*, vol. 98, no. 11, p. 114903, 2005.

[23] D. Anderson, M. Lisak, and T. Lewin, "Generalized criteria for microwave breakdown in air-filled waveguides," *J. Appl. Phys.*, vol. 65, no. 8, pp. 2935–2945, 1989.

[24] N. Shinohara, *Wireless Power Transfer Via Radiowaves*. NewYork, NY, USA: Wiley, 2014.

[25] K. G. Kato *et al.*, "Peer-peer phase-locking of two L-band industrial heating magnetrons," in *Proc. 5th IEEE Int. Vac. Electron. Conf. (IVEC)*, Apr. 2004, pp. 230–231.

[26] Z. Liu, X. Chen, M. Yang, K. Huang, and C. Liu, "Experimental studies on a 1-kW high-gain *S*-band magnetron amplifier with output phase control based on load–pull characterization," *IEEE Trans. Plasma Sci.*, vol. 46, no. 4, pp. 909–916, Apr. 2018.

Zhenlong Liu received the B.S. and M.S. degrees in electronics and information engineering from the School of Electronics and Information Engineering, Sichuan University, Chengdu, China, in 2010 and 2013, respectively, where he is currently pursuing the Ph.D. degree in communication systems and engineering.

His current research interests include injection-locking technology, microwave photonics, and high-power microwave combining.

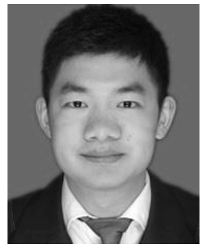

Xiaojie Chen received the B.S. degree in information counter technology from the College of National Defense Science and Technology, Southwest University of Science and Technology, Mianyang, China, in 2014. He is currently pursuing the master's degree in radio physics with the School of Electronics and Information Engineering, Sichuan University, Chengdu, China.

His current research interests include microwave engineering.

Menglin Yang received the B.S. degree in electronic information science and technology from the Chengdu University of Information Technology, Chengdu, China, in 2014. She is currently pursuing the master's degree in radio physics with the School of Electronics and Information Engineering, Sichuan University, Chengdu.

Her current research interests include microwave engineering.

Pengde Wu received the M.S. degree in measuring and testing technologies and instruments from the School of Automation Engineering, University of Electronic Science and Technology of China Engineering, Sichuan University, Chengdu, China, where he is currently pursuing the Ph.D. degree in radio physics with the School of Electronics and Information Engineering.

His current research interests include microwave circuits and high-power microwave combining.

Kama Huang received the M.S. and Ph.D. degrees in microwave theory and technology from the University of Electronic Science and Technology, Chengdu, China, in 1988 and 1991, respectively.

Since 1994, he has been a Professor with the School of Electronics and Information Engineering, Sichuan University, Chengdu, where he has been the Director of the School of Electronics and Information Engineering since 1997. In 1996, 1997, 1999, and 2001, he was a Visiting Scientist with the Scientific Research Center Vidhuk, Kiev, Ukraine, with the Institute of Biophysics CNR, Pisa, Italy, with the Technical University Vienna, Vienna, Austria, and also with Clemson University, Clemson, SC, USA, respectively.

Changjun Liu (M'07–SM'09) received the B.S. degree in applied physics from Hebei University, Baoding, China, in 1994, and the M.S. degree in radio physics and Ph.D. degree in biomedical engineering from Sichuan University, Chengdu, China, in 1997 and 2000, respectively.

From 2000 to 2001, he was a Post-Doctoral Researcher with Seoul National University, Seoul, South Korea. From 2006 to 2007, he was a Visiting Scholar with Ulm University, Ulm, Germany. Since 1997, he has been with the Department of Radio-Electronics, Sichuan University, where he has been a Professor since 2004. He has authored one book, one chapter in a book, and more than 100 articles. He holds more than 10 patents. His current research interests include microwave power combining of large-power vacuum components, microwave wireless power transmission, and microwave power industrial applications.

Dr. Liu was a recipient of several honors, such as the Outstanding Reviewer of the IEEE TRANSACTIONS ON MICROWAVE THEORY AND TECHNIQUES from 2006 to 2010, support from the MOE under the Program for New Century Excellent Talents in University, China, from 2012 to 2014, the Sichuan Province Outstanding Youth Fund from 2009 to 2012, and named by Sichuan Province as an Expert with Outstanding Contribution from 2008 to 2013. He serves on the editorial board of the *Chinese Journal of Applied Science*.